https://doi.org/10.5194/egusphere-2025-2295
Preprint. Discussion started: 10 June 2025

Emission Factors and Optical Properties of Black and Brown Carbon Emitted at a Mixed-Conifer Forest Prescribed Burn

James D.A. Butler,[1,2] Afsara Tasnia,[3] Deep Sengupta,[4] Nathan Kreisberg,[5] Kelley C. Barsanti,[3,6] Allen H. Goldstein,[1,5] Chelsea V. Preble,[1,2] Rebecca A. Sugrue,[1,2] Thomas W. Kirchstetter[1,2,*]

[1]Department of Civil and Environmental Engineering, University of California, Berkeley, Berkeley, California 94720

[2]Energy Technologies Area, Lawrence Berkeley National Laboratory, Berkeley, California 94720

[3]Department of Chemical and Environmental Engineering, Center for Environmental Research and Technology, University of California, Riverside, Riverside, California 92507

[4]Department of Environmental Science, Policy, and Management, University of California, Berkeley, Berkeley, California 94720

[5]Aerosol Dynamics Inc., Berkeley, California 94720

[6] Atmospheric Chemistry Observations and Modeling, U.S. National Science Foundation National Center for Atmospheric Research, Boulder, Colorado 80301

*Corresponding author email: twkirchstetter@lbl.gov

https://doi.org/10.5194/egusphere-2025-2295
Preprint. Discussion started: 10 June 2025

Abstract

Prescribed burning is a fuel management practice employed globally that emits carbonaceous aerosols that affect human health and perturb the global climate system. Aerosol black and brown carbon (BC and BrC) emission factors were calculated from ground and aloft smoke during prescribed burns at a mixed-conifer, montane forest site in the Sierra Nevada in California. BC emission factors were 0.52 ± 0.42 and 1.0 ± 0.48 g kg^{-1} for the smoldering and flaming combustion phases. MCE is a poor predictor of BC emission factor, in this study and published literature. We discuss limitations of using BC to $PM_{2.5}$ mass emission ratios to generate emissions inventories. Using BC emission factors measured in this study, we recommend BC to $PM_{2.5}$ ratios of 0.7% and 9.5% for the smoldering and flaming combustion. We calculated absorption Ångström exponents (AAE) based on multiwavelength absorption for BrC and BC of 6.26 and 0.67. Using the Delta-C method with a BrC-specific absorption cross-section, we estimate a smoldering combustion BrC emission factor of 7.0 ± 2.7 g kg^{-1}, nearly 14 and 7 times greater than the smoldering and flaming BC emission factors. Furthermore, we estimate that BrC would account for 23% and 82%, respectively, of the solar radiation absorbed by the smoldering smoke in the atmosphere integrated over the solar spectrum (300–2500 nm) and in the UV spectrum (300–400 nm), indicating that BrC affects tropospheric photochemistry in addition to atmospheric warming.

Key Figure

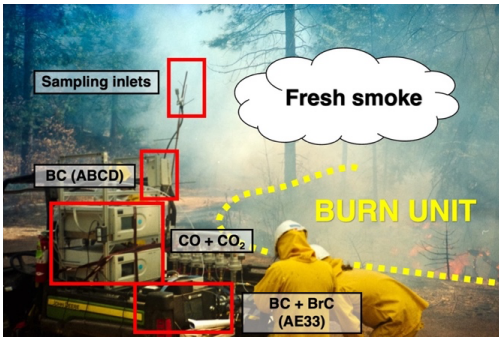

https://doi.org/10.5194/egusphere-2025-2295
Preprint. Discussion started: 10 June 2025

Keywords
Prescribed burn, black carbon, brown carbon, emission factor, light absorbing aerosol, wildland fire fuel consumption model

1 Introduction

Prescribed burns are controlled burns that consume excess and dead fuel in an ecosystem, like the duff, shrubs and dead biomass in the forest understory, or floor. In contrast, wildfires are uncontrolled burns that may consume both the understory and overstory, or canopy, of a forest and may spread to nearby property, endangering the homes and lives of people in the wildland urban interface. Routine prescribed burns, or other fuel management practices like mechanical thinning, reduce the risk and severity of wildfire ignition in forest ecosystems and increase the resistance to ecosystem transition (i.e., conversion of forest to shrubland) caused by wildfires (Steel et al., 2021; Wu et al., 2023).

Prescribed burns and wildfires emit fine particulate matter ($PM_{2.5}$), carbon monoxide (CO), carbon dioxide (CO_2), volatile organic compounds, and nitrogen oxides (Andreae, 2019; Urbanski, 2014; Urbanski et al., 2008; Wiedinmyer et al., 2006). Emitted $PM_{2.5}$ includes organic aerosol, some of which is light-absorbing brown carbon (BrC), and black carbon (BC). Whereas BC absorbs solar radiation broadly across the visible spectrum, BrC light absorption is highly wavelength dependent and strongest in the near-UV spectral region (Bond et al., 2004; Kirchstetter et al., 2004; Laskin et al., 2015). Due to their perturbation of the radiative balance of the atmosphere and short atmospheric residence time compared to CO_2, BC, and BrC are considered short-lived climate forcers (Feng et al., 2013; Kirchstetter and Thatcher, 2012; Zhang et al., 2020). Additionally, BC and BrC surface deposition in snowy climates reduces the solar reflectance of snow and may accelerate snow melt (Chelluboyina et al., 2024; Hadley and Kirchstetter, 2012; Kaspari et al., 2015; Yang et al., 2015). Human exposure to carbonaceous aerosols also has detrimental health effects including cardiovascular disease, lung cancer, adverse birth outcomes, and premature mortality (Dong et al., 2023; Grahame et al., 2014; Janssen et al., 2011). Wildland fires are a major source of pollution relevant to human exposure and account for one third of total $PM_{2.5}$ emissions in the U.S., with roughly equal contributions from prescribed burns and wildfires (Larkin et al., 2020).

https://doi.org/10.5194/egusphere-2025-2295
Preprint. Discussion started: 10 June 2025

Wildland fire modeling frameworks, or smoke models, estimate the amount of smoke emitted during burn events to create input emissions necessary for climate modeling, air pollution modeling, and health impact assessments (California Air Resources Board, 2020; Connolly et al., 2024; Cruz Núñez et al., 2014; Maji et al., 2024). Smoke emissions from wildland fires are estimated with fuel consumption models like Burnup, part of the First-Order Fire Effects Model (FOFEM), and CONSUME, part of the BlueSky Smoke Modeling Framework (Keane and Lutes, 2018; BlueSky Modeling Framework, 2024). Both smoke models compute total emissions of a pollutant by multiplying pollutant emission factors by the mass of fuel consumed during both the high intensity and low intensity stages of a burn event, which roughly correspond to the flaming and smoldering phases of a wildland fire.

The differences in fuel mass consumption and temperature in these phases affect the emission rate of pollutants, sometimes by an order of magnitude. In the flaming phase, fuel mass consumption and temperature are highest and combustion is more complete, while both are lower in the smoldering phase that is characterized by incomplete combustion (Urbanski, 2014). Flaming combustion generally has a higher emission rate of BC and a lower emission rate of BrC compared with smoldering combustion, while smoldering combustion is marked by higher emissions of CO and BrC (Chen et al., 2007). Experiments designed to quantify pollutant emissions must consider the placement of sampling instrumentation to capture these distinct combustion phases of a burn, with aerial sampling platforms more likely to capture a mixture of flaming and smoldering combustion due to the convective lofting of smoke caused by flaming combustion (Aurell et al., 2021). Ground-level smoke, on the other hand, tends to be dominated from smoldering combustion (Aurell and Gullett, 2013).

In this study, we conducted field sampling of pollutant emissions from prescribed burning of a mixed-conifer understory and computed BC emission factors, BrC emission factors, and aerosol absorption properties with ground and aerial sampling platforms. We investigate the relationship between BC emission factors and combustion conditions and, finding that the modified combustion efficiency (MCE) is a poor predictor of BC emission factor, propose a framework to aggregate emission factors by either flaming or smoldering conditions to convey the average value and variability of emission factors within these combustion regimes in fuel consumption models. We report BC/$PM_{2.5}$ ratios, or speciation profiles, for a mixed-conifer

https://doi.org/10.5194/egusphere-2025-2295
Preprint. Discussion started: 10 June 2025

understory prescribed burn. We then discuss how applying an incorrect BC/$PM_{2.5}$ ratio in wildland fire modeling frameworks may lead to large errors in BC emissions, using the ecosystem studied in this work as an example. We compute the absorption Ångström exponent (AAE) for the prescribed burn smoke aerosols, demonstrating that AAE is sensitive to the wavelengths used in its calculation, and present estimates of AAE separately for BC and BrC to estimate their contributions the solar radiation absorbed by the smoldering smoke in the atmosphere.

2 Materials and Methods

2.1 Field Measurements

Field measurements were made at the Blodgett Forest Research Station (38.915224, -120.662420), located 1370 meters above sea level on the western slope of the Sierra Nevada, 21 km east of Georgetown, CA. Prescribed burns were conducted in a mixed conifer forest, typical of montane ecosystems of the Sierra Nevada (North et al., 2016). Three forest units were burned in consecutive days in April 2021, as shown in Figure S1 in the Supporting Information (SI). The prescribed burn on the first day escaped the designated unit (A) and the burn was terminated early. The remainder of unit A was burned on the second day and units B and C were burned on the third and fourth days, respectively.

Prescribed burn smoke was measured using both a ground and an aerial sampling platform. The ground platform consisted of pollutant analyzers secured to a utility task vehicle stationed immediately downwind of the fire to capture fresh smoke two meters above ground level (see Figure S2). The ground platform was moved once each day as the burns progressed and winds shifted to be on service roads nearby the highest intensity burn activity and the aerial platform takeoff/landing location. Across the four days, there were nine ground sampling sessions: at two locations on each day, plus one “next-day” smoldering sample on the second day for burn unit A before ignition of the remaining unit. For the aerial platform, pollutant analyzers were attached to the unmanned aerial vehicle, a DJI Matrice 600 Pro hexacopter. Concurrent with ground sampling, the unmanned aerial vehicle was flown 23 times across the four days with at least five flights each day and a maximum of 10 flights on the third day. The average elevation

https://doi.org/10.5194/egusphere-2025-2295
Preprint. Discussion started: 10 June 2025

of aerial platform throughout sampling was 29 meters, with an average sampling elevation range of 16–42 meters across all flights.

BC, CO, and CO_2 were measured on both the ground and aerial sampling platforms. BC was measured using two filter-based aerosol absorption photometers: the Aerosol Magee Scientific aethalometer model AE33 with a 2.5 μm cyclone on the inlet on the ground platform and the custom-built Aerosol Black Carbon Detector (ABCD) on both the ground and aerial platforms (Caubel et al., 2018; Sugrue et al., 2024). The ABCD estimates BC concentration based on aerosol optical attenuation at 880 nm wavelength (λ). The AE33 also measures BC at λ=880 nm, in addition to aerosol optical attenuation at six other wavelengths. In particular, the AE33 reports the mass concentration UV-absorbing aerosol (UVPM) based on the optical attenuation at 370 nm. BrC concentration was estimated from these data as described below in Section 2.2. Collocating the AE33 with the ABCD on the ground enabled an analysis to express BC measured with the ABCD in terms of AE33 equivalence, also described below. CO and CO_2 were measured by non-dispersive infrared (NDIR) absorption photometry on the ground platform using Horiba models APMA370 and APCA370, respectively.(Tasnia et al., n.d.) CO and CO_2 were measured on the aerial platform with an electrochemical cell (Alphasense CO-B4) and NDIR sensor (PP Systems SBA-5), respectively. All instruments reported pollutant concentrations at 1 Hz frequency. Data were post-processed and validated prior to analysis using the quality assurance and control measures described in the SI, including pollutant concentration time-series alignment and loading artifact correction of BC concentrations measured with the ABCD.

2.2 Calculations

Light absorption by carbonaceous aerosols increases with decreasing wavelength, a trend that is often modeled as a power-law:

$$b_{abs}(\lambda) \propto \lambda^{-AAE} \qquad \text{(Equation 1)}$$

AAE was calculated by an ordinary least squares linear regression of the natural log transformation of λ and $b_{abs}(\lambda)$. Here, $b_{abs}(\lambda)$ (m^{-1}) was calculated by multiplying the wavelength-dependent, loading artifact-corrected, light-absorbing aerosol concentration reported by the AE33 by the wavelength-dependent mass absorption cross-section of BC on a filter (m^2

https://doi.org/10.5194/egusphere-2025-2295
Preprint. Discussion started: 10 June 2025

g^{-1}). Aerosol absorption was calculated per second and then averaged per minute with a 90% data completeness threshold applied at seven wavelengths measured by the ground aethalometer.

BrC mass concentrations were calculated using the Delta-C method, which estimates BrC as the difference between UVPM and BC concentrations in units of (μg m^{-3}):

$$BrC = UVPM - BC \quad \text{(Equation 2)}$$

The Delta-C method, as often applied in prior studies, projects BC absorption to the near UV wavelengths assuming $AAE_{BC} = 1$ and attributes excess light-absorption to BrC, where UVPM and, thus BrC, are assumed to have the same absorption cross-section as BC (18.47 m^2 g^{-1} at 370 nm) (Harrison et al., 2013; Huang et al., 2011; Stampfer et al., 2020; Wagstaff et al., 2022; Wang et al., 2010, 2011a, b). BrC concentration is thus operationally defined rather than an actual mass concentration. In this study, we use a BrC absorption cross-section empirically determined by Ivančič et al. (4.5 m^2 g^{-1} at 370 nm) and estimate the contribution of BC to each sample's spectral attenuation, $b_{abs,BC}(\lambda)$, by attributing all attenuation at 880 nm to BC and extrapolating to other wavelengths assuming $AAE_{BC} = 0.67$. This is the AAE_{BC} value determined in this study, as described below in Section 3.3.

Following the approach presented in Kirchstetter and Thatcher (2012), we computed the contribution of BrC to smoldering smoke aerosol absorption of solar radiation. The contribution of BrC to spectral absorption in each smoke sample, $b_{abs,BrC}(\lambda)$, is determined by subtracting the BC absorption from the total absorption:

$$b_{abs,BrC}(\lambda) = b_{abs}(\lambda) - b_{abs,BC}(\lambda) \quad \text{(Equation 3)}$$

Based on the apportionment of spectral absorption to BC and BrC, we compute the fraction of spectral radiation for smoldering smoke at each wavelength in the solar spectrum that would be absorbed by BrC:

$$f_{BrC} = \frac{b_{abs,BrC}(\lambda)}{b_{abs}(\lambda)} \quad \text{(Equation 4)}$$

Last, we compute the fraction of solar radiation that BrC in the smoldering smoke would absorb in the atmosphere:

$$F_{Brc} = \frac{\int_{\lambda_1}^{\lambda_2} f_{BrC}(\lambda) \cdot i(\lambda) d\lambda}{\int_{\lambda_1}^{\lambda_2} i(\lambda) d\lambda} \quad \text{(Equation 5)}$$

where $i(\lambda)$ is the clear sky air mass one global horizontal solar spectrum at the earth's surface (Levinson et al., 2010). We evaluate F_{BrC} using two sets of integration bounds (λ_1, λ_2): (1) across

https://doi.org/10.5194/egusphere-2025-2295
Preprint. Discussion started: 10 June 2025

the full solar irradiance spectrum from 300 to 2500 nm that is meaningful for atmospheric warming and (2) in the near-UV from 300 to 400 nm that is more relevant to tropospheric photochemistry (Li and Li, 2023; Mok et al., 2016).

The modified combustion efficiency (MCE) is typically used to assess the combustion completeness during biomass burning and was calculated as the mass fraction of fuel C emitted as CO_2 compared to CO_2 and CO (Ward and Radke, 1993):

$$MCE = \frac{\Delta CO_2}{\Delta CO_2 + \Delta CO} \quad \text{(Equation 6)}$$

Background-subtracted concentrations ΔCO and ΔCO_2 were calculated as the difference between measured concentrations and background concentrations, the latter of which were established separately for each of the four days of sampling (listed in Table S2). MCE is unitless, and a value of 0.9 is commonly used as a threshold to distinguish between flaming-dominated (MCE > 0.9) and smoldering-dominated (MCE < 0.9) combustion (Selimovic et al., 2018).

Fuel-based BC and BrC emission factors (EF_i) in units of grams BC and BrC emitted per kilogram fuel consumed (g kg^{-1}) were calculated by the carbon balance method:(Nelson Jr., 1982)

$$EF_i = \frac{w_c * V_m}{MW_C} \int_{t_0}^{t_1} \frac{\Delta C_i}{(\Delta CO + \Delta CO_2)} dt \quad \text{(Equation 7)}$$

where ΔC_i is the background-subtracted BC or BrC concentration (μg m^{-3}), w_c = 0.5 is the weight fraction of carbon in the biomass fuel (Urbanski, 2014), V_m is the molar volume of air and equal to 0.024 m^3 mol^{-1}, MW_c is the molar mass of carbon and equal to 12 g mol^{-1}, and ΔCO and ΔCO_2 are mixing ratios (ppm). Emission factors were calculated by integration of the background-subtracted pollutant concentrations over different time intervals. The integration bounds for the aerial emission factors were the start and end times of each flight, with a temporal basis equal to the total flight duration, or $t_1 - t_0$ in Eq. 4. Flight durations ranged from 4–22 minutes. For the ground emission factors, the start time (t_0) was when the aethalometer began collecting samples on a new filter spot and the attenuation (ATN) was zero. The end time (t_1) was when the filter became saturated at an ATN reached 100. At that point, the aethalometer advanced its filter tape. These integration bounds resulted in a ground sample temporal basis that corresponded to the ATN cycle of the aethalometer, which ranged from 2–36 minutes. A detailed discussion of the chosen temporal basis of the emission factors is provided in the SI.

https://doi.org/10.5194/egusphere-2025-2295
Preprint. Discussion started: 10 June 2025

3 Results and Discussion

3.1 Emission Factors

BC and BrC emission factors measured on the ground and aloft are presented in Table 1. Overall, the aerial platform measured smoke characterized by a higher modified combustion efficiency (MCE_{aerial} = 0.88 ± 0.05, average ± standard deviation) and nearly 2 times higher BC emission factor ($EF_{BC,aerial}$ = 0.92 ± 0.48 g kg^{-1}) than the smoke measured on the ground (MCE_{ground} = 0.83 ± 0.03; $EF_{BC,ground}$ = 0.47 ± 0.40 g kg^{-1}).

Table 1: Summary Statistics of Carbonaceous Aerosol Emission Factors and MCE (average ± standard deviation)

	Number of Samples	MCE	BC (g kg^{-1})	BrC (g kg^{-1})
Aerial samples	23	0.88 ± 0.05	0.92 ± 0.48	–
Ground samples	66	0.83 ± 0.03	0.47 ± 0.40	7.0 ± 2.7
Smoldering samples	77	<0.9	0.52 ± 0.42	–
Flaming samples	12	>0.9	1.0 ± 0.48	–
All samples	89	0.84 ± 0.04	0.59 ± 0.68	–

BC emission factors are plotted against MCE in Figure 1. Individual ground platform samples are plotted as orange circles and aerial samples are plotted as blue squares. Nearly all the smoke samples collected from the ground platform (64 of 66 ATN cycles) were associated with smoldering combustion (MCE < 0.9). A roughly equal number smoke samples collected aloft were associated with flaming-dominant combustion (10 flights) and smoldering-dominant combustion (13 flights). BC emission factors demonstrated a weak positive linear correlation (solid black line, r^2 = 0.11) against MCE values, with BC emission factors spanning an order of magnitude (0.11 to 1.70 g kg^{-1}) and MCE values ranging from 0.76 to 0.96. This relationship is similar to the weak positive linear trend reported by McMeeking et al. (2009) for a laboratory study (r^2 = 0.09), shown as a dashed black line in Figure 1a. In contrast, another laboratory study by Hosseini et al. (2013) reported a weak negative linear trend (dotted black line, r^2 = 0.10). The application of linear regression models to emission factor data would allow these field and laboratory studies to be scaled in fuel consumption models as a function of combustion

https://doi.org/10.5194/egusphere-2025-2295
Preprint. Discussion started: 10 June 2025

248 conditions and/or fire intensity (Burling et al., 2011; May et al., 2014; Ottmar, 2014; Selimovic
249 et al., 2018; Urbanski, 2014). However, given the very low coefficients of determination from
250 this work and previous laboratory studies ($r^2 < 0.15$), MCE is not a strong predictor of the BC
251 emission factor for smoke model estimates.

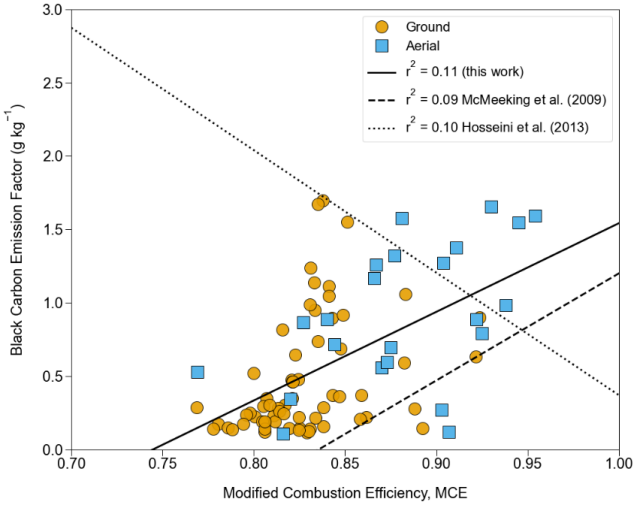

252

253 Figure 1: BC emission factors plotted against modified combustion efficiency for all samples.
254 Symbology designates the ground (circles) and aerial (squares) measurement platforms. All
255 samples fit with a linear regression model and compared to previous laboratory linear models of
256 BC emission factors as a function of MCE (Hosseini et al., 2013; McMeeking et al., 2009).
257

258 **3.2 Emissions Modeling in Fuel Consumption Models**

259 BC emission factor distributions for flaming (MCE>0.9) and smoldering (MCE<0.9)
260 conditions are presented in Figure 2. These combustion categories were chosen to match how
261 smoke models calculate emissions, often with combustion-phase dependent emission factors.
262 Fuel consumption models (e.g., Burnup, CONSUME) compute the total fuel consumed
263 separately during flaming and smoldering combustion phases of a burn. Smoke models then
264 apply the appropriate EFs, with either one EF for flaming combustion and one EF for smoldering
265 combustion (e.g., FOFEM), or using a linear model like presented in Figure 1a in which the
266 calculated MCE in the fuel consumption model is used to obtain the corresponding EF. The
267 average BC emission factors measured during flaming combustion conditions in this study were
268 nearly 2 times greater than those measured during smoldering conditions: $EF_{BC,flaming} = 1.0 \pm$

https://doi.org/10.5194/egusphere-2025-2295
Preprint. Discussion started: 10 June 2025

269 0.48 g kg^{-1} versus $EF_{BC,\ smoldering}$ = 0.52 ± 0.42, with similar magnitude the average emissions
270 factors for aerial and ground samples reported above.
271

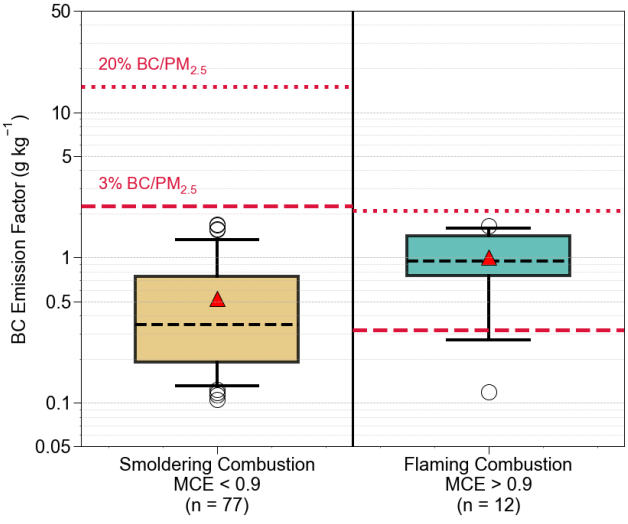

272
273 Figure 2: BC emission factors categorized into smoldering combustion (MCE < 0.9) and flaming
274 combustion (MCE > 0.9) phases for input into fuel consumption. Boxes represent the
275 interquartile range and tails the 5th and 95th percentile. The median is provided as the black
276 dashed line across the box, the average as a red triangle, and outliers as open circles. Speciation
277 profile-derived BC emission factors for 3% and 20% BC/$PM_{2.5}$ for each combustion phase are
278 plotted as red horizontal dashed and dotted lines, respectively. Note the logarithmic scale on the
279 y-axis.
280

281 Also included in Figure 2 are BC emission factors calculated with the FOFEM
282 methodology as a fraction of $PM_{2.5}$ emission factors from Burling et al. (2011) for a mixed-
283 conifer understory prescribed burn (Burling et al., 2011; Lutes, 2020). These BC emission factors
284 are plotted as horizontal lines across each combustion regime in Figure 2 and represent values
285 assumed in the most recent federal and California BC inventories. The 2020 National Emissions
286 Inventory (dashed line) assumes a 3% BC/$PM_{2.5}$ mass ratio for all wildland fire sources,
287 including prescribed burns and wildfires (US Environmental Protection Agency, 2023). The 2013
288 California BC Emissions Inventory (dotted line) assumes a 20% BC/$PM_{2.5}$ mass ratio for
289 prescribed burns (California Air Resources Board, 2016). These BC/$PM_{2.5}$ mass ratios—or BC

https://doi.org/10.5194/egusphere-2025-2295
Preprint. Discussion started: 10 June 2025

speciation profiles—are known to be highly uncertain (Chow et al., 2011). For example, in the EPA SPECIATE v5.3 database, prescribed burn BC/$PM_{2.5}$ mass ratios vary from 3–11% and for uncontrolled forest fire or forest fuel types between 0.8–80% (SPECIATE, 2025).

The difference between the average flaming and smoldering BC emission factors measured in this study and the BC emission factors estimated from BC/$PM_{2.5}$ ratios reveals the current limitation in using the latter methodology in wildland fire modeling frameworks to estimate BC emissions. $PM_{2.5}$ emission rates for mixed-conifer forests and many other ecosystems are higher under smoldering combustion than under flaming combustion, the opposite of BC emission rates (Burling et al., 2011; Chen et al., 2007). As a result, BC emission rates are erroneously predicted to be greater under smoldering combustion. The speciation profiles assumed in the federal and California inventories overestimate BC emission factors under smoldering combustion for this type of burn by a factor 4 and 29, respectively. Under flaming combustion, the California inventory overestimates BC emission rates by a factor of 2, whereas the federal inventory underestimates by 0.3. Dividing the average field BC emission factors in this study by the literature $PM_{2.5}$ emission factor indicates that a more appropriate BC speciation profile for a mixed-conifer understory prescribed burn would be 0.7% and 9.5% for the smoldering and flaming combustion phases, respectively.

3.3 Optical Properties and Apportionment of Aerosol Solar Radiation Absorption

BrC emission factors were computed based on ground-level smoke measurements with the multiwavelength aethalometer, most of which (64 of 66 samples) were during smoldering-dominated combustion. There as a very weak positive linear relationship ($r^2 = 0.06$) between BrC emission factors and MCE (Figure 3). The study average BrC emission factor was 7.0 ± 2.7 g kg^{-1}. It is worth noting that this BrC emission factor, computed as described in Section 2.2 based on an absorption cross-section specific to BrC, is 4.4 times greater than the emission factor calculated using the more traditional Delta-C method, where the absorption-cross section of BrC is operationally defined as equal to the absorption cross-section of BC.

https://doi.org/10.5194/egusphere-2025-2295
Preprint. Discussion started: 10 June 2025

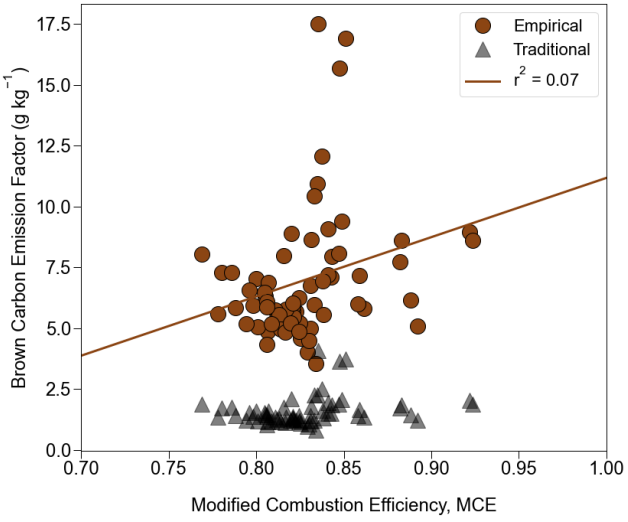

Figure 3: Ground BrC emission factors computed using the Delta-C method with a BrC-specific mass absorption cross-section (denoted as Empirical and shown with brown circles) and the more traditional approach using an operationally defined BrC mass absorption cross-section equal to that of BC (denoted as Traditional and shown with grey triangles) plotted against modified combustion efficiency. The solid brown line shows the linear regression for the BrC emission factors calculated with the empirical approach.

Study-average spectral absorption curves are plotted in Figure 4. A power-law fit to the data over all aethalometer wavelengths from 370–950 nm is shown in Figure 4a. The absorption data are fit with two trend lines in Figure 4b: an extrapolation of the power law fit to the near-IR data at 880 and 950 nm to illustrate the BC contribution to total absorption, $b_{abs,BC}(\lambda)$, and a power law fit of the BrC contribution to absorption, $b_{abs,BrC}(\lambda)$, which extends from mid-visible wavelengths to the near-UV, calculated using Eq. 3. The AAE given by the power law exponent reported in Figure 4a is 2.32 (1.35, 3.29; 95% confidence interval), indicating a significant contribution of BrC to total absorption. The power law fits in Figure 4b yield AAE_{BrC} = 6.26 (5.37, 7.13) and AAE_{BC} = 0.67. For comparison, El Asmar et al. (2024) found similar overall AAE = 1.89 (range of 1.31–3.32) and a lower average AAE_{BrC} = 5.00 (range of 3.19–7.43) for prescribed burns in southeastern US measured 0–8 hours downwind with the same model multiwavelength aethalometer used in this study. The AAE_{BrC} for western wildfires measured with a photoacoustic spectrometer by Zeng et al. (2022) was also comparable (2.07 ± 1.01;

https://doi.org/10.5194/egusphere-2025-2295
Preprint. Discussion started: 10 June 2025

339 average ± standard deviation). Mie theory predicts that AAE_{BC} = 1 for particle diameters less
340 than 10 nm and AAE_{BC} < 1 for particle diameters greater than ~0.2 µm (Wang et al., 2016),
341 suggesting that the bulk of sampled aerosols had a diameter greater than 0.2 µm and less than 2.5
342 µm, since a $PM_{2.5}$ cyclone was placed on the sampling inlet.
343

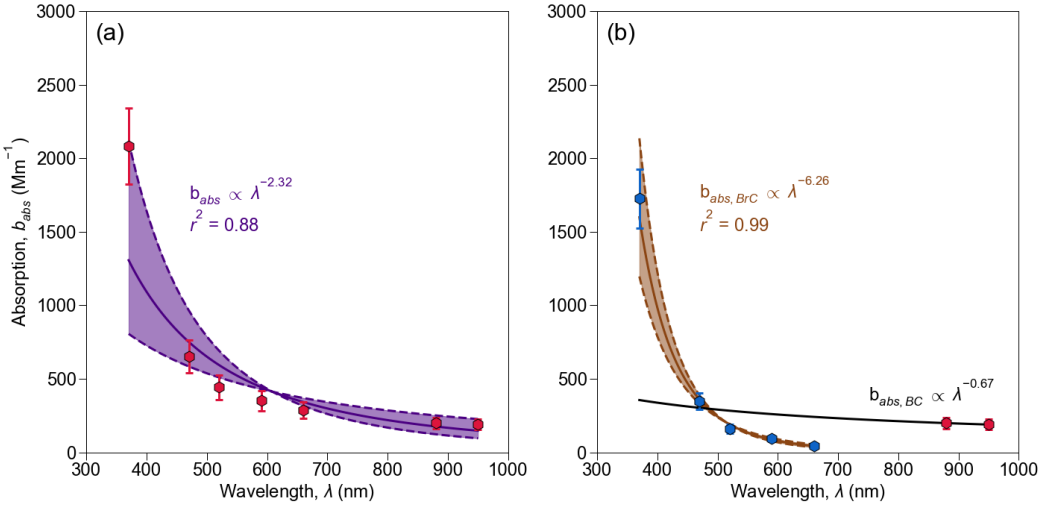

344
345 Figure 4: Average 1-minute absorption at seven wavelengths measured by the ground
346 aethalometer plotted as red hexagons, with error bars representing 95% confidence intervals. (a)
347 Power-law fit of the average absorption curve at all wavelengths with an AAE = 2.32 and a 95%
348 confidence interval displayed by the shading between the dashed curves. (b) Power-law fit of the
349 BrC average absorption curve (λ = 370, 470, 520, 590, and 660 nm; blue circles) with an AAE_{BrC}
350 = 3.43 and a 95% confidence interval displayed by the shading between the dashed curves and
351 the BC average absorptions (λ = 880, 950 nm; red hexagons) with an AAE_{BC} = 0.67.
352

353 Whereas the absorption cross-section of BrC is much lower than that of BC over the near-
354 IR to near-UV portion of the solar spectrum, smoldering smoke emits much more BrC than BC:
355 7.0 ± 2.7 gBrC kg^{-1} versus 0.52 ± 0.42 gBC kg^{-1}. Consequently, using Equation 5 and shown in
356 Figure S10, we estimate that BrC and BC would account for 23% and 77% of incoming solar
357 radiation absorbed by the smoldering smoke in the atmosphere (integrated from 300 to 2500
358 nm). Furthermore, BrC would contribute 82% of the aerosol absorption of solar radiation at
359 wavelengths below 400 nm and, therefore, may affect tropospheric photochemistry.

https://doi.org/10.5194/egusphere-2025-2295
Preprint. Discussion started: 10 June 2025

AAE values reported in the literature are computed using different approaches. For example, AAE is commonly derived from data at only two wavelengths and those wavelengths differ from study to study, which makes direct comparison among studies challenging. To illustrate this point, we calculated AAE values on 1-minute absorption data from the current study using three wavelength pairs that approximate prior work. Table 2 reports power law fitting of (i) 370 and 880 nm to approximate the wavelengths in a photoacoustic extinctiometer, (ii) 470 and 660 nm to approximate a continuous light absorption photometer, and (iii) 470 and 880 nm to approximate the satellite based AERONET.

Table 2: Measured and Nearest Aethalometer Wavelengths to Calculate the Absorption Ångström Exponent (AAE)

Carbonaceous Aerosol Measurement Method	**Example Studies**	**Measured Wavelengths, λ (nm)**	**Nearest Aethalometer Wavelengths, λ (nm)**	**AAE, Average ± Standard Deviation**
Aethalometer (Magee Scientific AE33)	This Work (Butler et al.) El Asmar et al. (2024)	370, 470, 520, 590, 660, 880, 950	—	2.55 ± 0.43
Photoacoustic spectrometer (Droplet Technologies PAX)	Selimovic et al. (2018) Zeng et al. (2022)	401, 870	370, 880	2.97 ± 0.54
Continuous light absorption photometer	Marsavin et al. (2023)	467, 652	470, 660	2.82 ± 0.59
Satellite (AERONET)	Cazorla et al. (2013) Feng et al. (2013) Wang et al. (2016) Bian et al. (2020)	440, 870	470, 880	2.15 ± 0.37

The 1-minute average AAE for the three wavelength pairs are listed in the rightmost column of Table 2. The 370, 880 and 470, 880 wavelength pairs have a 16% and 11% greater value than the seven-wavelength power law fit in this work, whereas the 440, 870 wavelength pair a 16% lesser value. These differences in average AAE indicate the uncertainty in interstudy

https://doi.org/10.5194/egusphere-2025-2295
Preprint. Discussion started: 10 June 2025

comparison is approximately ± 15%. Distributions of the coefficient of determination (r^2) for each approach are also presented in Figure S11. A power law fit of 1-minute average data at all seven wavelengths ($AAE_{7\lambda}$) yielded the highest average coefficient of determination (r^2 = 0.88), followed closely by fitting data at only 370 and 880 nm (r^2 = 0.87). The lower average r^2 values for power law fitting of data at 470 and 660 nm (r^2 = 0.71) and 470 and 880 nm (r^2 = 0.60) suggest that the AAE values determined from these approaches are not as certain.

4 Conclusion

Fuel-based BC and BrC emission factors were calculated by the carbon balance method with semi-continuous monitoring of a BC, CO, and CO_2 on ground and aerial platforms for four days of prescribed burns. Aerial platform BC emission factors were measured under both flaming and smoldering combustion, whereas ground platform BC and BrC emission factors skewed towards almost entirely under smoldering combustion conditions. AAE, an aerosol optical property, was similarly quantified for smoldering combustion. BC emission factors were found to be poorly represented by a linear regression model based on MCE and were 2 times higher under flaming combustion than smoldering combustion. In addition, BC emission factors may be used in smoke models to improve wildland fire emissions inventories. BrC emission factors, estimated using a BrC-specific absorption cross-section, were nearly 14 and 7 times greater than the smoldering and flaming BC emission factors, respectively. The study-average AAE indicated significant BrC absorption, especially in the near-UV spectrum, indicating that BrC is a significant contributor to biomass smoke absorption of solar radiation. The AAE_{BrC} reported here may be parametrized in global earth systems models to represent the contribution of BrC to total aerosol absorption of incoming shortwave radiation for mixed-conifer prescribed burning (Saleh, 2020).

In future work, deployment of a multiwavelength aethalometer on the aerial platform, would allow for Delta-C and AAE analyses to estimate BrC emission factors and optical properties under flaming combustion. Multiwavelength aerosol absorption measurements on an aerial platform across a wide range of combustion conditions would yield more representative BrC emission factors and AAE values, which would inform how to model BrC emissions during different combustion phases in fuel consumption models. Studies that quantify health impacts of

https://doi.org/10.5194/egusphere-2025-2295
Preprint. Discussion started: 10 June 2025

prescribed burn smoke with a chemical transport model will benefit from fuel-based emission factors in this work and could determine the exposure concentrations of BC and BrC in $PM_{2.5}$. The overall radiative effects of BC and BrC remains uncertain due to large uncertainties in global emissions inventories from wildland fires sources (Bond et al., 2013). Further improvements in bottom-up carbonaceous aerosol emissions inventories would constrain satellite retrievals of aerosol optical depth used to model aerosol scattering and absorption in global climate models.

To mitigate the health and climate impacts of BC and BrC emissions, prescribed burns will be critical to promote climate resilient, fire-adapted forest ecosystems. Prescribed burns consume less fuel per burned area than wildfires by a factor of 2–4, emit less greenhouse gases and climate pollutants, and have less severe smoke health impacts (Kelp et al., 2023; Kiely et al., 2024; Ottmar, 2014). Further partnership between government agencies, private land owners, and tribal nations will likely increase the frequency and effectiveness of prescribed burns (Miller et al., 2020). Indigenous fire stewardship should be centered in this aim, which uses controlled fire to change fire regimes in ecosystems to adapt to climate change, encourage certain species growth, and increase resources to sustain indigenous knowledge, cultural practices, and traditions (Lake and Christianson, 2019). As prescribed burns increase in prevalence, continued field measurements of emission factors with state-of-the-science platforms should focus on generating emission factors for ecosystems and wildland fire activity globally.

Author Contribution

James D.A. Butler: Conceptualization, Data Curation, Formal Analysis, Investigation, Methodology, Resources, Visualization, Writing – original draft, Writing – review and editing.
Afsara Tasnia: Data Curation, Investigation, Methodology, Resources, Writing – review and editing.
Deep Sengupta: Data Curation, Investigation, Methodology, Resources.
Nathan Kreisberg: Data Curation, Investigation, Methodology, Resources, Writing – review and editing.
Kelley C. Barsanti: Conceptualization, Funding Acquisition, Methodology, Project Administration, Supervision, Writing – review and editing.

https://doi.org/10.5194/egusphere-2025-2295
Preprint. Discussion started: 10 June 2025

Allen H Goldstein: Conceptualization, Funding Acquisition, Methodology, Project Administration, Supervision, Writing – review and editing.
Chelsea V. Preble: Conceptualization, Methodology, Resources, Writing – review and editing.
Rebecca A. Sugrue: Resources, Writing – review and editing.
Thomas W. Kirchstetter: Conceptualization, Funding Acquisition, Methodology, Writing – original draft, Writing – review and editing.

Competing interests

We declare that co-author Barsanti is on the editorial board of the journal *Atmospheric Chemistry and Physics.*

Code/Data Availability

Data and code available upon request.

Acknowledgement

This work was supported by the California Air Resources Board (CARB) under contract 19RD008 and the California Department of Forestry and Fire Protection (CAL FIRE). Butler, Kirchstetter, Preble, and Sugrue also acknowledge support of the Department of Energy under Contract No. DEAC02-05CH11231. The statements and conclusions herein are those of the authors and do not necessarily reflect the views of the project sponsors. We thank Ariel Roughton, Rob York, John Battles, Scott Stephens and the staff of the Blodgett Forest Research Station for their work to conduct the prescribed burns, feed and house the research team, and ensure safety when taking field measurements; Coty Jen for her feedback on early analyses; Drew Hill for his assistance on the Delta-C methodology; Adam Wise for development of the photographs in Key Figure, Figure S2, and Figure S9; and Robert Harley for his review of early drafts.

https://doi.org/10.5194/egusphere-2025-2295
Preprint. Discussion started: 10 June 2025

References

Andreae, M. O.: Emission of trace gases and aerosols from biomass burning – an updated assessment, Atmospheric Chemistry and Physics, 19, 8523–8546, https://doi.org/10.5194/acp-19-8523-2019, 2019.

Aurell, J. and Gullett, B. K.: Emission Factors from Aerial and Ground Measurements of Field and Laboratory Forest Burns in the Southeastern U.S.: PM2.5, Black and Brown Carbon, VOC, and PCDD/PCDF, Environ. Sci. Technol., 47, 8443–8452, https://doi.org/10.1021/es402101k, 2013.

Aurell, J., Gullett, B., Holder, A., Kiros, F., Mitchell, W., Watts, A., and Ottmar, R.: Wildland fire emission sampling at Fishlake National Forest, Utah using an unmanned aircraft system, Atmospheric Environment, 247, 118193, https://doi.org/10.1016/j.atmosenv.2021.118193, 2021.

Bian, Q., Ford, B., Pierce, J. R., and Kreidenweis, S. M.: A Decadal Climatology of Chemical, Physical, and Optical Properties of Ambient Smoke in the Western and Southeastern United States, Journal of Geophysical Research: Atmospheres, 125, e2019JD031372, https://doi.org/10.1029/2019JD031372, 2020.

Bond, T. C., Streets, D. G., Yarber, K. F., Nelson, S. M., Woo, J.-H., and Klimont, Z.: A technology-based global inventory of black and organic carbon emissions from combustion, Journal of Geophysical Research: Atmospheres, 109, https://doi.org/10.1029/2003JD003697, 2004.

Bond, T. C., Doherty, S. J., Fahey, D. W., Forster, P. M., Berntsen, T., DeAngelo, B. J., Flanner, M. G., Ghan, S., Kärcher, B., Koch, D., Kinne, S., Kondo, Y., Quinn, P. K., Sarofim, M. C., Schultz, M. G., Schulz, M., Venkataraman, C., Zhang, H., Zhang, S., Bellouin, N., Guttikunda, S. K., Hopke, P. K., Jacobson, M. Z., Kaiser, J. W., Klimont, Z., Lohmann, U., Schwarz, J. P., Shindell, D., Storelvmo, T., Warren, S. G., and Zender, C. S.: Bounding the role of black carbon in the climate system: A scientific assessment, Journal of Geophysical Research: Atmospheres, 118, 5380–5552, https://doi.org/10.1002/jgrd.50171, 2013.

Burling, I. R., Yokelson, R. J., Akagi, S. K., Urbanski, S. P., Wold, C. E., Griffith, D. W. T., Johnson, T. J., Reardon, J., and Weise, D. R.: Airborne and ground-based measurements of the trace gases and particles emitted by prescribed fires in the United States, Atmospheric Chemistry and Physics, 11, 12197–12216, https://doi.org/10.5194/acp-11-12197-2011, 2011.

California Air Resources Board: California's Black Carbon Emission Inventory–Technical Support Document, 2016.

California Air Resources Board: Greenhouse Gas Emissions of Contemporary Wildfire, Prescribed Fire, and Forest Management Activities, California Air Resources Board, Sacramento, CA, 2020.

Caubel, J. J., Cados, T. E., and Kirchstetter, T. W.: A new black carbon sensor for dense air quality monitoring networks, Sensors, 18, 738, https://doi.org/10.3390/s18030738, 2018.

https://doi.org/10.5194/egusphere-2025-2295
Preprint. Discussion started: 10 June 2025

Cazorla, A., Bahadur, R., Suski, K. J., Cahill, J. F., Chand, D., Schmid, B., Ramanathan, V., and Prather, K. A.: Relating aerosol absorption due to soot, organic carbon, and dust to emission sources determined from in-situ chemical measurements, Atmospheric Chemistry and Physics, 13, 9337–9350, https://doi.org/10.5194/acp-13-9337-2013, 2013.

Chelluboyina, G. S., Kapoor, T. S., and Chakrabarty, R. K.: Dark brown carbon from wildfires: a potent snow radiative forcing agent?, npj Clim Atmos Sci, 7, 1–10, https://doi.org/10.1038/s41612-024-00738-7, 2024.

Chen, L.-W. A., Moosmüller, H., Arnott, W. P., Chow, J. C., Watson, J. G., Susott, R. A., Babbitt, R. E., Wold, C. E., Lincoln, E. N., and Hao, W. M.: Emissions from Laboratory Combustion of Wildland Fuels: Emission Factors and Source Profiles, Environ. Sci. Technol., 41, 4317–4325, https://doi.org/10.1021/es062364i, 2007.

Chow, J. C., Watson, J. G., Lowenthal, D. H., Antony Chen, L.-W., and Motallebi, N.: PM2.5 source profiles for black and organic carbon emission inventories, Atmospheric Environment, 45, 5407–5414, https://doi.org/10.1016/j.atmosenv.2011.07.011, 2011.

Connolly, R., Marlier, M. E., Garcia-Gonzales, D. A., Wilkins, J., Su, J., Bekker, C., Jung, J., Bonilla, E., Burnett, R. T., Zhu, Y., and Jerrett, M.: Mortality attributable to PM2.5 from wildland fires in California from 2008 to 2018, Science Advances, 10, eadl1252, https://doi.org/10.1126/sciadv.adl1252, 2024.

Cruz Núñez, X., Villers Ruiz, L., and Gay García, C.: Black carbon and organic carbon emissions from wildfires in Mexico, Atmósfera, 27, 165–172, https://doi.org/10.1016/S0187-6236(14)71107-5, 2014.

Dong, Q., Meng, X., Gong, J., and Zhu, T.: A review of advances in black carbon exposure assessment and health effects, CSB, 69, 703–716, https://doi.org/10.1360/TB-2023-0409, 2023.

El Asmar, R., Li, Z., Tanner, D. J., Hu, Y., O'Neill, S., Huey, L. G., Odman, M. T., and Weber, R. J.: A multi-site passive approach to studying the emissions and evolution of smoke from prescribed fires, Atmospheric Chemistry and Physics, 24, 12749–12773, https://doi.org/10.5194/acp-24-12749-2024, 2024.

Feng, Y., Ramanathan, V., and Kotamarthi, V. R.: Brown carbon: a significant atmospheric absorber of solar radiation?, Atmospheric Chemistry and Physics, 13, 8607–8621, https://doi.org/10.5194/acp-13-8607-2013, 2013.

Grahame, T. J., Klemm, R., and Schlesinger, R. B.: Public health and components of particulate matter: The changing assessment of black carbon, Journal of the Air & Waste Management Association, 64, 620–660, https://doi.org/10.1080/10962247.2014.912692, 2014.

Hadley, O. L. and Kirchstetter, T. W.: Black-carbon reduction of snow albedo, Nature Clim Change, 2, 437–440, https://doi.org/10.1038/nclimate1433, 2012.

https://doi.org/10.5194/egusphere-2025-2295
Preprint. Discussion started: 10 June 2025

Harrison, R. M., Beddows, D. C. S., Jones, A. M., Calvo, A., Alves, C., and Pio, C.: An evaluation of some issues regarding the use of aethalometers to measure woodsmoke concentrations, Atmospheric Environment, 80, 540–548, https://doi.org/10.1016/j.atmosenv.2013.08.026, 2013.

Hosseini, S., Urbanski, S. P., Dixit, P., Qi, L., Burling, I. R., Yokelson, R. J., Johnson, T. J., Shrivastava, M., Jung, H. S., Weise, D. R., Miller, J. W., and Cocker III, D. R.: Laboratory characterization of PM emissions from combustion of wildland biomass fuels, Journal of Geophysical Research: Atmospheres, 118, 9914–9929, https://doi.org/10.1002/jgrd.50481, 2013.

Huang, J., Hopke, P. K., Choi, H.-D., Laing, J. R., Cui, H., Zananski, T. J., Chandrasekaran, S. R., Rattigan, O. V., and Holsen, T. M.: Mercury (Hg) emissions from domestic biomass combustion for space heating, Chemosphere, 84, 1694–1699, https://doi.org/10.1016/j.chemosphere.2011.04.078, 2011.

Ivančič, M., Gregorič, A., Lavrič, G., Alföldy, B., Ježek, I., Hasheminassab, S., Pakbin, P., Ahangar, F., Sowlat, M., Boddeker, S., and Rigler, M.: Two-year-long high-time-resolution apportionment of primary and secondary carbonaceous aerosols in the Los Angeles Basin using an advanced total carbon–black carbon (TC-BC(λ)) method, Science of The Total Environment, 848, 157606, https://doi.org/10.1016/j.scitotenv.2022.157606, 2022.

Janssen, N. A. H., Hoek, G., Simic-Lawson, M., Fischer, P., van Bree, L., ten Brink, H., Keuken, M., Atkinson, R. W., Anderson, H. R., Brunekreef, B., and Cassee, F. R.: Black carbon as an additional indicator of the adverse health effects of airborne particles compared with PM10 and PM2.5, Environ Health Perspect, 119, 1691–1699, https://doi.org/10.1289/ehp.1003369, 2011.

Kaspari, S., McKenzie Skiles, S., Delaney, I., Dixon, D., and Painter, T. H.: Accelerated glacier melt on Snow Dome, Mount Olympus, Washington, USA, due to deposition of black carbon and mineral dust from wildfire, Journal of Geophysical Research: Atmospheres, 120, 2793–2807, https://doi.org/10.1002/2014JD022676, 2015.

Keane, R. E. and Lutes, D.: First-Order Fire Effects Model (FOFEM), in: Encyclopedia of Wildfires and Wildland-Urban Interface (WUI) Fires, edited by: Manzello, S. L., Springer International Publishing, Cham, 1–5, https://doi.org/10.1007/978-3-319-51727-8_74-1, 2018.

Kelp, M. M., Carroll, M. C., Liu, T., Yantosca, R. M., Hockenberry, H. E., and Mickley, L. J.: Prescribed Burns as a Tool to Mitigate Future Wildfire Smoke Exposure: Lessons for States and Rural Environmental Justice Communities, Earth's Future, 11, e2022EF003468, https://doi.org/10.1029/2022EF003468, 2023.

Kiely, L., Neyestani, S. E., Binte-Shahid, S., York, R. A., Porter, W. C., and Barsanti, K. C.: California Case Study of Wildfires and Prescribed Burns: PM2.5 Emissions, Concentrations, and Implications for Human Health, Environ. Sci. Technol., 58, 5210–5219, https://doi.org/10.1021/acs.est.3c06421, 2024.

https://doi.org/10.5194/egusphere-2025-2295
Preprint. Discussion started: 10 June 2025

573 Kirchstetter, T. W. and Thatcher, T. L.: Contribution of organic carbon to wood smoke particulate
574 matter absorption of solar radiation, Atmospheric Chemistry and Physics, 12, 6067–6072,
575 https://doi.org/10.5194/acp-12-6067-2012, 2012.

576 Kirchstetter, T. W., Novakov, T., and Hobbs, P. V.: Evidence that the spectral dependence of light
577 absorption by aerosols is affected by organic carbon, Journal of Geophysical Research:
578 Atmospheres, 109, https://doi.org/10.1029/2004JD004999, 2004.

579 Lake, F. K. and Christianson, A. C.: Indigenous Fire Stewardship, in: Encyclopedia of Wildfires
580 and Wildland-Urban Interface (WUI) Fires, edited by: Manzello, S. L., Springer International
581 Publishing, Cham, 1–9, https://doi.org/10.1007/978-3-319-51727-8_225-1, 2019.

582 Larkin, N. K., Raffuse, S. M., Huang, S., Pavlovic, N., Lahm, P., and Rao, V.: The
583 Comprehensive Fire Information Reconciled Emissions (CFIRE) inventory: Wildland fire
584 emissions developed for the 2011 and 2014 U.S. National Emissions Inventory, Journal of the
585 Air & Waste Management Association, 70, 1165–1185,
586 https://doi.org/10.1080/10962247.2020.1802365, 2020.

587 BlueSky Modeling Framework: https://www.airfire.org/data/bluesky, last access: 12 November
588 2024.

589 Laskin, A., Laskin, J., and Nizkorodov, S. A.: Chemistry of Atmospheric Brown Carbon, Chem.
590 Rev., 115, 4335–4382, https://doi.org/10.1021/cr5006167, 2015.

591 Levinson, R., Akbari, H., and Berdahl, P.: Measuring solar reflectance—Part I: Defining a metric
592 that accurately predicts solar heat gain, Solar Energy, 84, 1717–1744,
593 https://doi.org/10.1016/j.solener.2010.04.018, 2010.

594 Li, J. and Li, Y.: Ozone deterioration over North China plain caused by light absorption of black
595 carbon and organic carbon, Atmospheric Environment, 313, 120048,
596 https://doi.org/10.1016/j.atmosenv.2023.120048, 2023.

597 Lutes, D. C.: FOFEM 6.7 User Guide, United States Forest Service, 2020.

598 Maji, K. J., Li, Z., Vaidyanathan, A., Hu, Y., Stowell, J. D., Milando, C., Wellenius, G., Kinney,
599 P. L., Russell, A. G., and Odman, M. T.: Estimated Impacts of Prescribed Fires on Air Quality
600 and Premature Deaths in Georgia and Surrounding Areas in the US, 2015–2020, Environ. Sci.
601 Technol., https://doi.org/10.1021/acs.est.4c00890, 2024.

602 Marsavin, A., Gageldonk, R. van, Bernays, N., May, N. W., Jaffe, D. A., and Fry, J. L.: Optical
603 properties of biomass burning aerosol during the 2021 Oregon fire season: comparison between
604 wild and prescribed fires, Environ. Sci.: Atmos., 3, 608–626,
605 https://doi.org/10.1039/D2EA00118G, 2023.

606 May, A. A., McMeeking, G. R., Lee, T., Taylor, J. W., Craven, J. S., Burling, I., Sullivan, A. P.,
607 Akagi, S., Collett, J. L., Flynn, M., Coe, H., Urbanski, S. P., Seinfeld, J. H., Yokelson, R. J., and
608 Kreidenweis, S. M.: Aerosol emissions from prescribed fires in the United States: A synthesis of

https://doi.org/10.5194/egusphere-2025-2295
Preprint. Discussion started: 10 June 2025

laboratory and aircraft measurements, Journal of Geophysical Research: Atmospheres, 119, 11,826-11,849, https://doi.org/10.1002/2014JD021848, 2014.

McMeeking, G. R., Kreidenweis, S. M., Baker, S., Carrico, C. M., Chow, J. C., Collett, J. L., Hao, W. M., Holden, A. S., Kirchstetter, T. W., Malm, W. C., Moosmüller, H., Sullivan, A. P., and Wold, C. E.: Emissions of trace gases and aerosols during the open combustion of biomass in the laboratory, Journal of Geophysical Research: Atmospheres, 114, https://doi.org/10.1029/2009JD011836, 2009.

Miller, R. K., Field, C. B., and Mach, K. J.: Barriers and enablers for prescribed burns for wildfire management in California, Nat Sustain, 3, 101–109, https://doi.org/10.1038/s41893-019-0451-7, 2020.

Mok, J., Krotkov, N. A., Arola, A., Torres, O., Jethva, H., Andrade, M., Labow, G., Eck, T. F., Li, Z., Dickerson, R. R., Stenchikov, G. L., Osipov, S., and Ren, X.: Impacts of brown carbon from biomass burning on surface UV and ozone photochemistry in the Amazon Basin, Sci Rep, 6, 36940, https://doi.org/10.1038/srep36940, 2016.

Nelson Jr., R. M.: An evaluation of the carbon balance technique for estimating emission factors and fuel consumption in forest fires, Res. Pap. SE-231. Asheville, NC: U.S. Department of Agriculture, Forest Service, Southeastern Forest Experiment Station, 231, 9, https://doi.org/10.2737/SE-RP-231, 1982.

North, M., Collins, B., Safford, H., and Stephenson, N.: Montane Forests, in: Ecosystems of California, University of California Press, 553–578, 2016.

Ottmar, R. D.: Wildland fire emissions, carbon, and climate: Modeling fuel consumption, Forest Ecology and Management, 317, 41–50, https://doi.org/10.1016/j.foreco.2013.06.010, 2014.

Saleh, R.: From Measurements to Models: Toward Accurate Representation of Brown Carbon in Climate Calculations, Curr Pollution Rep, 6, 90–104, https://doi.org/10.1007/s40726-020-00139-3, 2020.

Selimovic, V., Yokelson, R. J., Warneke, C., Roberts, J. M., de Gouw, J., Reardon, J., and Griffith, D. W. T.: Aerosol optical properties and trace gas emissions by PAX and OP-FTIR for laboratory-simulated western US wildfires during FIREX, Atmospheric Chemistry and Physics, 18, 2929–2948, https://doi.org/10.5194/acp-18-2929-2018, 2018.

Stampfer, O., Austin, E., Ganuelas, T., Fiander, T., Seto, E., and Karr, C. J.: Use of low-cost PM monitors and a multi-wavelength aethalometer to characterize PM2.5 in the Yakama Nation reservation, Atmospheric Environment, 224, 117292, https://doi.org/10.1016/j.atmosenv.2020.117292, 2020.

Steel, Z. L., Foster, D., Coppoletta, M., Lydersen, J. M., Stephens, S. L., Paudel, A., Markwith, S. H., Merriam, K., and Collins, B. M.: Ecological resilience and vegetation transition in the face

https://doi.org/10.5194/egusphere-2025-2295
Preprint. Discussion started: 10 June 2025

of two successive large wildfires, Journal of Ecology, 109, 3340–3355, https://doi.org/10.1111/1365-2745.13764, 2021.

Sugrue, R. A., Preble, C. V., Butler, J. D. A., Redon-Gabel, A. J., Marconi, P., Shetty, K. D., Hill, L. A. L., Amezcua-Smith, A. M., Lukanov, B. R., and Kirchstetter, T. W.: The value of adding black carbon to community monitoring of particulate matter, Atmospheric Environment, 325, 120434, https://doi.org/10.1016/j.atmosenv.2024.120434, 2024.

Tasnia, A., Lara, G., Foster, D., Sengupta, D., Butler, J., Kirchstetter, T. W., York, R., Kreisberg, N., Goldstein, A. G., Battles, J. J., and Barsanti, K. C.: Fuel Loadings Prove the Critical Constraint for Smoke Predictions using FOFEM as applied to a Mixed Conifer Forest in California, ACS ES&T Air, n.d.

Urbanski, S.: Wildland fire emissions, carbon, and climate: Emission factors, Forest Ecology and Management, 317, 51–60, https://doi.org/10.1016/j.foreco.2013.05.045, 2014.

Urbanski, S. P., Hao, W. M., and Baker, S.: Chapter 4 Chemical Composition of Wildland Fire Emissions, in: Developments in Environmental Science, vol. 8, edited by: Bytnerowicz, A., Arbaugh, M. J., Riebau, A. R., and Andersen, C., Elsevier, 79–107, https://doi.org/10.1016/S1474-8177(08)00004-1, 2008.

US Environmental Protection Agency: 2020 National Emissions Inventory Technical Support Document: Fires –Wild, Prescribed, and Agricultural Field Burning, US Environmental Protection Agency, Research Triangle Park, NC, 2023.

SPECIATE: https://www.epa.gov/air-emissions-modeling/speciate-0, last access: 16 January 2025.

Wagstaff, M., Henderson, S. B., McLean, K. E., and Brauer, M.: Development of methods for citizen scientist mapping of residential woodsmoke in small communities, Journal of Environmental Management, 311, 114788, https://doi.org/10.1016/j.jenvman.2022.114788, 2022.

Wang, X., Heald, C. L., Sedlacek, A. J., de Sá, S. S., Martin, S. T., Alexander, M. L., Watson, T. B., Aiken, A. C., Springston, S. R., and Artaxo, P.: Deriving brown carbon from multiwavelength absorption measurements: method and application to AERONET and Aethalometer observations, Atmospheric Chemistry and Physics, 16, 12733–12752, https://doi.org/10.5194/acp-16-12733-2016, 2016.

Wang, Y., Huang, J., Zananski, T. J., Hopke, P. K., and Holsen, T. M.: Impacts of the Canadian Forest Fires on Atmospheric Mercury and Carbonaceous Particles in Northern New York, Environ. Sci. Technol., 44, 8435–8440, https://doi.org/10.1021/es1024806, 2010.

Wang, Y., Hopke, P. K., Rattigan, O. V., Xia, X., Chalupa, D. C., and Utell, M. J.: Characterization of Residential Wood Combustion Particles Using the Two-Wavelength Aethalometer, Environ. Sci. Technol., 45, 7387–7393, https://doi.org/10.1021/es2013984, 2011a.

https://doi.org/10.5194/egusphere-2025-2295
Preprint. Discussion started: 10 June 2025

679 Wang, Y., Hopke, P. K., and Utell, M. J.: Urban-scale Spatial-temporal Variability of Black
680 Carbon and Winter Residential Wood Combustion Particles, Aerosol Air Qual. Res., 11, 473–
681 481, https://doi.org/10.4209/aaqr.2011.01.0005, 2011b.

682 Ward, D. E. and Radke, L. F.: Emissions Measurements from Vegetation Fires: A Comparative
683 Evaluation of Methods and Results, in: Fire in the Environmentl: The Ecological, Atmospheric,
684 and Climatic Importance of Vegetation Fires, John Wiley & Sons Ltd., 53–76, 1993.

685 Wiedinmyer, C., Quayle, B., Geron, C., Belote, A., McKenzie, D., Zhang, X., O'Neill, S., and
686 Wynne, K. K.: Estimating emissions from fires in North America for air quality modeling,
687 Atmospheric Environment, 40, 3419–3432, https://doi.org/10.1016/j.atmosenv.2006.02.010,
688 2006.

689 Wu, X., Sverdrup, E., Mastrandrea, M. D., Wara, M. W., and Wager, S.: Low-intensity fires
690 mitigate the risk of high-intensity wildfires in California's forests, Science Advances, 9,
691 eadi4123, https://doi.org/10.1126/sciadv.adi4123, 2023.

692 Yang, S., Xu, B., Cao, J., Zender, C. S., and Wang, M.: Climate effect of black carbon aerosol in
693 a Tibetan Plateau glacier, Atmospheric Environment, 111, 71–78,
694 https://doi.org/10.1016/j.atmosenv.2015.03.016, 2015.

695 Zeng, L., Dibb, J., Scheuer, E., Katich, J. M., Schwarz, J. P., Bourgeois, I., Peischl, J., Ryerson,
696 T., Warneke, C., Perring, A. E., Diskin, G. S., DiGangi, J. P., Nowak, J. B., Moore, R. H.,
697 Wiggins, E. B., Pagonis, D., Guo, H., Campuzano-Jost, P., Jimenez, J. L., Xu, L., and Weber, R.
698 J.: Characteristics and evolution of brown carbon in western United States wildfires,
699 Atmospheric Chemistry and Physics, 22, 8009–8036, https://doi.org/10.5194/acp-22-8009-2022,
700 2022.

701 Zhang, A., Wang, Y., Zhang, Y., Weber, R. J., Song, Y., Ke, Z., and Zou, Y.: Modeling the global
702 radiative effect of brown carbon: a potentially larger heating source in the tropical free
703 troposphere than black carbon, Atmospheric Chemistry and Physics, 20, 1901–1920,
704 https://doi.org/10.5194/acp-20-1901-2020, 2020.

705